Using Remote Sensing and Machine Learning to Monitor Urban Growth in Didcot, United Kindgom

Candidate Number: 183781
Supervisor: Prof Seb Oliver
Word Count: 7126
Last Updated: May 20, 2020

University of Sussex

Abstract

Over-population of Earth is a key concern for governments of countries all over the world, especially in developing countries. United Nations has addressed this and emphasises sustainable growth as an important goal for the future. Modern day remote sensing, using Earth observing satellites, in conjunction with machine learning methods, can assist with helping cities grow in a sustainable and planned fashion. This report focuses on pixel-based classification of land covers and applies them to the town of Didcot in Oxfordshire, United Kingdom. Classification maps of 2013, 2015 and 2020 were successful and showed a noticeable increase in built-up/urban areas over this seven year time frame. Growth of urban areas in and around Didcot from 2013 to 2020 being the primary focus saw an increase by 80% overall. Random Forest Classifier was the ensemble algorithm used and the model was found to have a 97.6% accuracy with the training data. However the classification for 2015 was not viable to extract data concerning built-up areas from. To gain more accurate results, more training data could be used or more sophisticated algorithms could be employed. Object-based classification has been shown to be a more superior method for land cover classifications in multiple reports and so could be a suitable improvement for future classifications of the area. The population of Didcot will approximately double within ten years and so planning policies will need to be put in the subsequent years. Further classification maps of the area will assist with careful growth and sustainable development of the town and it's infrastructure.

Contents

List of Tables

List of Figures

Preface

Chapter 1 is an introduction that was written by myself. Chapter 2 gives background material about relevant topics of the project. All of this material was written by myself. Chapter 3 details the methods used to acquire the results desired in the project. The code used was adapted from code written by Edward Salakpi. I added to this code heavily to make it relevant to my work and furthered it. This code is expected to be uploaded in GitHub so that it is publicly available to be used for future endeavours. Chapter 4 contains all results obtained during the project including figures and tables. All of this is my original work. Chapter 5 and 6 are simply an interpretation of the results and a conclusion. Both are my own work.

Glossary

NDVI	**N**ormalised **D**ifference **V**egetation **I**ndex
NDWI	**N**ormalised **D**ifference **W**ater **I**ndex
MNDWI	**M**odified **N**ormalised **D**ifference **W**ater **I**ndex
NDBI	**N**ormalised **D**ifference **B**uilt-up **I**ndex
OBIA	**O**bject **B**ased **I**mage **A**nalysis
SDG	**S**ustainable **D**evelopment **G**oals
DN	**D**igital **N**umber
NIR	**N**ear **I**nfra**R**ed
SWIR	**S**hort**W**ave **I**nfra**R**ed
QA	**Q**uality **A**ssessment
NaN	**N**ot a **N**umber
OLI	**O**perational **L**and **I**mager

Chapter 1

Introduction

According to the United Nations, the global population of Earth is estimated to reach ten billion by the year 2050, with seven billion of these people living in urban areas (United Nations, 2019b). This is a 75% increase from today's four billion. The cities of today are facing unprecedented challenges because of the sheer amount of people living in them. The cities of tomorrow will be much busier, have a larger footprint and will require a larger amount of resources to be kept running. To make sure they have longevity and can maintain their population effectively, these megacities will have to be built in a sustainable manner. Sustainability has been defined as "meeting the needs of the present without compromising the ability of future generations to meet their own needs" (United Nations, 2020). This is a concept that has been made increasingly more significant to the world in the past few decades due to the growing concern of climate change and other environmental issues. Since this population growth will occur relatively quickly, action will be needed in the subsequent decades to prepare. To secure a better future the UN have addressed this issue in goal #11 of the sustainable development goals (SDG). This aims at making cities and human settlements inclusive, safe, resilient and sustainable (United Nations, 2019a). The SDG are a general manifesto of goals to be achieved so that a better quality of life can be a common standard among all inhabitants of the planet and for future generations.

No ambitious endeavour is completed without the innovation and utilisation of technology - and this one is no different. Monitoring urban areas and planning how they will grow is key. This requires two important components; real-time, large scale remote sensing methods and further machine learning techniques to process the data into useful information. In particular, this project uses and studies satellite images of the Earth's surface in conjunction with pixel-based classification. Machine learning techniques are used to create a classification model that produces information applicable to the real-world. For example, they allow for the visualisation of how specific land cover types change over time. In addition, the data can be used to monitor other environments that require some attention, in particular; Nature. The considerable growth of the domain of man-made structures means the destruction of forests, plains, jungles, etc. the impact on the ecology of Earth will need to be closely studied as we expand our territory. This is of upmost importance as many existential and moral questions arise from this subject.

The goal of this project is to explore and use machine learning techniques, combined with remote sensing images, to primarily monitor and analyse the development of built-up areas, as well as observing other land cover types. More specialised indices will be made to focus on the profile of a single land cover. Also the suitability of the techniques used will be evaluated. The focal point of this project was to apply this all to a local area of known urban growth and classification maps over a seven year period using multi-temporal spatial

data. Conclusions are then drawn focusing on the future of the area and the factors that might contribute to its growth. The success of the applied machine learning techniques is commented upon and as well as possible improvements that could be made.

Chapter 2

Background

2.1 Land Cover Classification

An image of the Earth's surface will contain within it many different types of land cover. For example an image may contain a city, dotted with parks, with forest surrounding it. The differences in the colour of the pixels that contain these land covers will be a good indicator of what they are, as well as the shape and general layout of the objects. To build a classification of the image, all of these different land covers must be differentiated from one another and named. There are two main modern classification techniques: pixel-based classification and object based image analysis (OBIA). OBIA is more accurate in many cases as it uses a more advanced algorithm that takes into account multiple characteristic factors of the objects in the image. However I have used pixel-based classification which is done by using the pixel values in the image. All classification relies on the handling of the digital numbers that are fundamental to each pixel. Each digital number (DN) describes the amount of flux received from that area. Lower values correlate to a lower radiance (Phiri and Morgenroth, 2017). Furthermore, images have to be corrected by removing clouds from the image because they will simply clutter results with unwanted information. Ultimately, classification is carried out by mathematically grouping pixels into classes that each represent a different type of land cover. Pixels that are selected to be in a class are more similar than to those in other classes. This is important because not all DN values that make up a section of forest will be the same. So constructing the classes to contain a more complete range of values that are valid for that class is a key part of the process as this can determine how accurate the classification will be. This is where the limitations of this classification method start to arise: a DN value may be present in more than one type of land cover and so it becomes difficult to distinguish the two classes. For example, some buildings may be made of a material that is spectrally similar to the surrounding landscape. This is where other characteristics could be taken into consideration which OBIA does to great effect. However, indices do provide an effective way to solve this issue to an extent. Moreover, pixel-based classification can come in two forms: supervised and unsupervised. The most significant difference between the two being that supervised classification involves manually labelling samples from the image to be used to train the model for classification. On the other hand, unsupervised classification relies on the generation of groups of similar pixels to be the basis for the classification, without hand-picked training data (Geography, 2020).

2.2 Satellite Earth Observation (EO)

The satellite images that were used in this project were taken by the Landsat 8 satellite; the eighth satellite in the Landsat program, developed as a joint collaboration between

	Bands	Wavelength (micrometers)	Resolution (meters)
Landsat 8 Operational Land Imager (OLI) and Thermal Infrared Sensor (TIRS) Launched February 11, 2013	Band 1 - Coastal aerosol	0.43 - 0.45	30
	Band 2 - Blue	0.45 - 0.51	30
	Band 3 - Green	0.53 - 0.59	30
	Band 4 - Red	0.64 - 0.67	30
	Band 5 - Near Infrared (NIR)	0.85 - 0.88	30
	Band 6 - SWIR 1	1.57 - 1.65	30
	Band 7 - SWIR 2	2.11 - 2.29	30
	Band 8 - Panchromatic	0.50 - 0.68	15
	Band 9 - Cirrus	1.36 - 1.38	30
	Band 10 - Thermal Infrared (TIRS) 1	10.60 - 11.19	100
	Band 11 - Thermal Infrared (TIRS) 2	11.50 - 12.51	100

Figure 2.1: A table showing all of the operating bands of the Landsat 8 satellite. Source: https://www.usgs.gov/media/images/landsat-8-band-designations.

NASA and United States Geological Survey (USGS). The instruments are more advanced than Landsat 7 (the previous instalment in the program) and include the OLI (Operational Land Imager) and TIRS (Thermal Infrared Sensor). These sensors can detect signals in eleven distinct bands, where each band is a range of wavelengths (see Figure 2.1) (NASA, 2020). The TIRS detects within Bands 10 and 11 which unsurprisingly lie in the infrared wavelength range and are of no concern to this project. Whereas the OLI is responsible for all other nine bands. The bands that are of great use to this project are: band 2 (Green), band 3 (Blue), band 4 (Red), band 5 (NIR) and band 6 (SWIR). Superimposing the images taken in the red, green and blue bands gives a true colour image. These true colour composites are the basic element on which I built my classifications upon, as they give a good view of the Earth's surface. The other two band in the infrared region are used within calculations for additional features. The resolution for these bands is 30m, as it is for all the other bands (except band 8). Moreover, all bands and images are retrieved from earthexplorer.usgs.gov. It is available to the public and is free.

2.3 Satellite EO Indices

Using the images produced by EO satellites, the following NDVI, NDBI and MNDWI can be calculated to improve the performance of the classification and to study specific land covers.

2.3.1 NDVI

Bands 4 and 5 are used to calculate the NDVI (Normalised Difference Vegetation Index). The NDVI is very useful for looking at natural environments that are densely populated with plants. It can detect how densely populated the area is with plants or how healthy they are. Healthy plants will strongly absorb visible light with a wavelength 0.4-0.7 microns to be used in photosynthesis. Whereas NIR (Near Infrared) light from 0.7-1.1 microns is reflected by the cell structure of leaves. So the less visible light that is detected, the more has been absorbed by the plant meaning that it is healthy (NASA, 2000). However the more NIR that is detected, the more has been reflected by the leaves meaning that the

plant/area is densely populated (with leaves). Using equation 2.1 and inputting the values in these wavelength ranges, the NDVI can be calculated. NDVI values range from -1 to 1, where -1 to 0 represents water bodies and 0 to 1 represents land covered in vegetation. The denser the vegetation, the greater the value (Kshetri, 2018). Mapping the NDVI can provide a useful visualisation of how human settlement has reduced the size of an area covered with vegetation or perhaps how air pollution caused by humans has affected the environment around it.

$$NDVI = \frac{NIR - RED}{NIR + RED} \tag{2.1}$$

2.3.2 NDBI

The NDBI (Normalised Difference Built-up Index) enhances the visibility of urban environments and bare soil which both have a higher reflectance in SWIR than NIR due to the properties of common construction materials. Water does not reflect in the Infrared region and natural environments will reflect more NIR than SWIR. Therefore the formula for NDBI uses SWIR and NIR (see equation 2.2) so that urban areas will give a positive value, water gives a zero value and natural environments give negative values. This index can be used for watershed run-off predictions and planning land usage (ArcGIS, 2020). Values for the NDBI range between -1 and +1 (Kshetri, 2018).

$$NDBI = \frac{SWIR - NIR}{SWIR + NIR} \tag{2.2}$$

2.3.3 MNDWI

The MNDWI (Modified Normalised Difference Water Index) is a modified version of the NDWI and is used to highlight water bodies. The older NDWI (McFEETERS, 1996) used the NIR and SWIR bands in its calculation which enhanced the water related features of an image. However this was modified to become the MNDWI by Xu, 2006 and uses green (Band 3) and SWIR (Band 6) instead (see equation 2.3). The older NDWI often mixed up built-up areas as water and therefore over-estimated the amount of water, whereas the MNDWI highlights open water while reducing sources of noise such as built-up areas, vegetation and soil. Again values range from -1 to +1 where water will be greater than 0.5, whereas built-up areas and vegetation will have small values around zero (Kshetri, 2018).

$$NDWI = \frac{GREEN - SWIR}{GREEN + SWIR} \tag{2.3}$$

2.4 Examples of Classification

There are multiple papers that review classification of urban areas and assess a specific area. For example, Al-Bilbisi, 2019 focused on the capital city of Jordan; Amman found that the urban area increased by 61.73% in the last three decades from 149km^2 in 1987 to 237.86 km^2 in 2017. He concluded that vertical construction is highly recommended to keep the growth somewhat sustainable. This type of insight using reliable and sophisticated data can be very advantageous when assisting in city planning. Countries such as China that already have a very large population will have great need for this. Ming et al., 2016 produced classification maps in Changping, Beijing, China using the Random Forest Classifier in combination with another algorithm. The study focused on the optimisation of the classification by using these algorithms together. Random Forest Classifier is the same machine learning classifier that was used in this project. In addition to monitoring urban development, classification on forests and other natural environments can provide good insight into effects of area and even population of different species. For example, Xie

et al., 2019 published a paper in 2019 exploring the accuracy of different techniques on classifying by specific tree species. For some species, the classification accuracy exceeded 92% whilst other were around 85%. These machine learning applications are fairly new and need to be developed more as their use could prove very useful for conservation and ecology worldwide.

Chapter 3

Methodology

3.1 Selecting Area

At the beginning of the project, my main goal was to use machine learning to create a classification map of an urban area that had not been looked at before. Obviously the area that was going to be my target had to have gone through a significant amount of urban growth in recent years so that the change of land covers over time was noticeable. However it could not be too large of an area so that it was not too much to handle at first as choosing something like a large city, although maybe be more interesting, would be very time consuming and potentially overwhelming. The town of Didcot in Oxfordshire was my selection as it is near the village in which I live and there has been quite substantial growth in recent years. Multiple housing estate projects and large commercial construction developments have been completed along with an increase in population to the town. Therefore there must be a noticeable change of land cover types in the area, especially as the surrounding land is largely dominated by farmland and some woodland which provides a good contrast to urban environments.

3.2 Image Data

As previously stated the satellite images that are used in this project were retrieved from earthexplorer.usgs.gov and come in the form of .tif files. The Landsat 8 satellite takes images of the Earth's surface in relation to a grid system of rows and columns. Each raw image is a single tile that makes up the grid. However each tile that I have used are approximately 7900 x 7800 pixels, which corresponds to 237 x 234 km. This is quite a large area of land and so to see the area of interest, it has to be zoomed in on specific coordinates. I zoomed in to my area of interest and noted the x and y ranges of values that contain the town of Didcot and an appropriate amount of surrounding area. The surrounding area fits in a couple of peripheral villages that have seen a lot of growth as well as a large scientific campus. Also there is a sufficient amount of farmland and other land covers in the image to be used.

I initially selected images from 01 FEB 2014, 17 JUN 2017 and 20 APR 2019. This caused problems because the images were from different times of years which affected the image in a way that made the classifications very inaccurate in 2017 and 2019. It was important for them all to be from the same month, ideally within a couple of weeks from each other and from years separated by regular time intervals. However, this criterion, along with the low amount of cloud coverage required, limited the number of suitable images quite significantly. The images that most closely followed my criteria were the following: 08 JUN 2013, 09 APR 2015, 19 MAY 2018 and 22 APR 2020. Since the overall time range

of the images increased, an extra image had to be included to get more desirable time intervals.

Zip files for each year were downloaded and extracted, each containing two quality assessment files (QA files), bands 1 - 7 (.tif images) and some other miscellaneous files. The QA files that is relevant is the pixel_qa band file which contains various flags that describe the following quality conditions: cloud, cloud confidence, cirrus cloud confidence, cloud shadow and snow/ice and water. This file is very useful when removing cloud from the images which is explained in more detail in the cloud correction section.

3.3 Class Extraction

QGIS is a free and open-source geographic information system software that enables geospatial data to be viewed and processed in a variety of ways. Within the application, the image for each band can be viewed and compiled to produce the true colour image that will be the basis for the classifications. Building a virtual raster with the red, green and blue bands creates a true colour image. Then grouping pixel clusters in this image and assigning them to different classes will be the beginning of constructing the data needed for the classification model.

QGIS enabled polygons to be drawn around a group of pixels on an RGB image where the groups were attributed to different classes. The spatial information for each polygon is contained within a shape file. The file contains geometric data that when applied to an image will produce pixel clusters that will be used for training the model. I gave the shape file three fields: ID, Class and Class Name. The ID is an intrinsic and unique value to each item on the list. The Class Name and Class are essentially the same title that denotes which class the item belongs to, however Class is just an integer and Class Name is text. Built up areas such as residential, commercial and industrial districts are Class 1. Roads are also included in Class 1. Farming fields are Class 2 and woodlands are Class 3. There is very little woodland around the town as most of the land is dominated by farming fields. These three classes were the ones that I started with but found that the classification could be more accurate and detailed, so two more classes were added. Class 4 is dedicated to bare soils and dry land and finally Class 5 is for open water bodies. After establishing a list of classes, I used the polygon tool to draw a shape around a group of pixels that represented a type of land cover, being careful not to include any pixels that may be adjacent and not belonging to the same class. Then I attached the polygon shape to the matching class. In doing this, each pixel that fell inside of the polygon now was attributed to class. 22 items are in the shape file layer, each describing the geometric areas for pixels to be extracted from later.

3.3.1 Extraction of Training Data

The geometry data contained within the output file made by QGIS allows clusters of pixel to be taken from the same location. Then using a for loop in Python, pixels within each polygon were extracted for each band and then applies them to the relevant band in a data frame. So the pixel values are organised per band under the headings: Blue Band, Green Band, Red Band, NIR Band and SWIR band. This populated data frame is then exported as a .csv file so that it can be imported easily into the classification notebook.

3.4 Feature Engineering

The data frame from the class extraction file had features for all the different bands, however I created three more features in the data frame; NDVI, MNDWI and NDVI. These features take the values of a pixel from two different bands in the data frame and calculate a value for the relevant index by inputting those values into a formula. Each one can provide specific and clear information on a specific land cover, which is made obvious by the names. More importantly, these additional features will help make the model more accurate since they are precise at locating specific types of land cover. A greater number of indices means that the classification will become increasingly more accurate. Furthermore, any values outside of the the valid range of -1 to +1 were removed from the data sets.

3.4.1 NDVI

The images that map the NDVI over the area that I have used for my classification are comprised of dark blues, green and yellow colours. The brighter/more yellow the pixel, the higher the NDVI value of that pixel is and therefore the vegetation in that pixel is healthier. Since the majority of the vegetation in the image are crops in farm fields, they will all be of similar density since crops are planted fairly uniformly. Data from bands 4 and 5 are used to calculate this index (see equation 3.1).

$$NDVI = \frac{Band5 - Band4}{Band5 + Band4} \tag{3.1}$$

3.4.2 NDBI

There are a few useful indices that can be used to directly look at the built-up areas in particular, for example; NDBI, Built-up Index (BU) and Urban Index (UI). The most fundamental being the NDBI. The formula uses the fact that built-up area reflect more SWIR (Band 6) than NIR (Band 5) (see equation 3.2).

$$NDBI = \frac{Band6 - Band5}{Band6 + Band5} \tag{3.2}$$

3.4.3 MNDWI

The MNDWI is used to monitor the changes of water bodies and uses values from band 3 and 6 (see equation 3.3). Values range from -1 to +1 where water will be greater than 0.5, whereas built-up areas and vegetation will have small values around zero.

$$MNDWI = \frac{Band3 - Band6}{Band3 + Band6} \tag{3.3}$$

3.5 Cloud Correction

Before classifying the image, clouds that obscure the land have to be removed from the image so that they do not affect the classification. Ultimately this was done by replacing the pixels values that represented non-clear pixels (clouds) with values that corresponded to no data, which I made to be -999. The QA files contained a different set of values for each pixel that described whether the atmosphere was clear or not. If it was clear, then the values were to be 322, 386, 834, 898 and 1346. So the arrays that described the image for each band were edited to remove any pixels that did not have these values in the QA file. I also did the same for the water values; 324, 388, 836, 900, 1348 which initially got

treated as undesired values. There is a river running through the images and so this was quite important. Otherwise the water in the image would be incorrectly classified (usually as no data). Therefore any pixels that had cloud or any other undesired features would be removed from the image. In addition, the values for each pixel after radiometric correction was supposed to be between 1 and 0. Just to remove outliers that would cause problems, the value of any pixel outside of this range was changed to be NaN (Not a Number). All NaN values were later changed to -999 values which the machine learning model then treated as a value with no data. In the final classification they are simply represented by grey pixels.

With the new corrected arrays for each band, they were then exported to a .tif file so that I could import them later when constructing the data frame for the classifications and other features. This step is very important as the clouds can interfere with the machine learning so that the classification would be inaccurate and more cluttered.

3.6 Training and Testing Data

The classification relies on the machine learning techniques that teach the computer to differentiate pixels in the images from one another. This is done by loading training data from the extracted classes that contain the pixel values and which classes they belong to. This will enable a mapping function to learnt that can then be applied to all of the pixels in the image to put each pixel value/data point (x value) in a class (y value). So the training data is used to train the model and the test data is used to test how well it works. I split the data into training data and testing data by using the train_test_split feature in the sklearn module. This split the array of data in to random data subsets.

3.6.1 Training Model

Training the model is mainly done by using an ensemble algorithm called Random Forest Classifier within the sklearn module. Ensemble algorithms use multiple algorithms for classifying objects together in the form of multiple decision trees. Random Forest Classifier creates a set of decision trees based off of the training data that it is given, which it then aggregates the results to decide the class of the object. An aggregate of multiple decision trees is preferable to a single one that can be susceptible to noise. The reduction of noise from combining results gives a more accurate result (Patel, 2017). Therefore this algorithm is a robust and reliable way to train the data and is used quite often for classification machine learning.

3.7 Classification of Data from All Time Points

All of the bands have been corrected to not include clouds and so I created another data frame with eight columns - five for each band and three for the indices. The corrected images were converted into arrays and loaded into the data frame. Each array had 120000 entries but 900 of these entries were labelled as no data because of cloud. Then using the trained model on these data points, predictions were computed for each pixel in the arrays. Finally the predicted classes for each pixel were reshaped into an 400x300 image. Each class was assigned a colour and visualised in to an image.

Chapter 4

Results

4.1 Urban Area Development

(a) True colour image of Didcot in 2013.

(b) True colour image of Didcot in 2015.

(c) True colour image of Didcot in 2018.

(d) True colour image of Didcot in 2020.

Figure 4.1: Comparison of all true colour images focused on Didcot from 2013, 2015, 2018 and 2020.

Figure 4.1 shows true colour composite images of the town of Didcot in the years 2013, 2015, 2018 and 2020. These images were created by compiling data from bands 2, 3 and 4 captured by the OLI instrument on board Landsat 8. The exposure of the images has

been increased to allow for clearer observation. At the centre of the image is the town of Didcot and in the bottom-left is Harwell Campus. A few smaller villages can be seen to the south and west of Didcot and it is clear that the dominant class of land cover is in fact farmland. There is a slight offset between the images caused by the irregular size and position of the original tile that these images are a part of. I changed the coordinates that were used to zoom in to try and make the images more uniform.

4.2 Classification of Land Cover Analysis

Figure 4.2 shows the land cover classification maps for the town of Didcot that are the result of supervised classification techniques. The five distinct colours that populate the image represent each class of land cover. A key is included to show which colours are attached to each class. The land cover that is most abundant in each frame (except 2015) is the farmland. This is also quite evident from the true colour composite images.

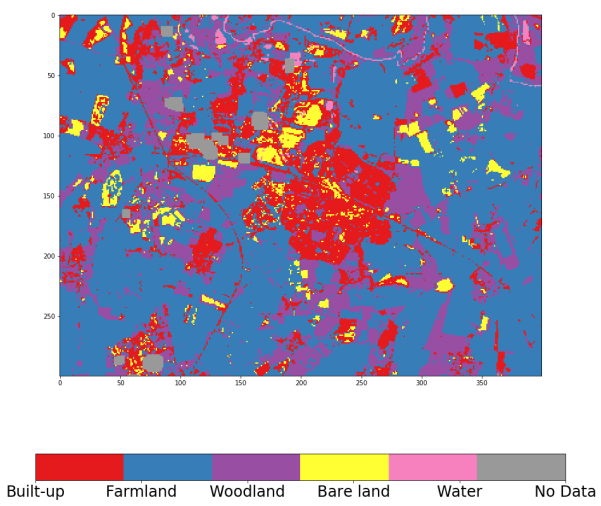

(a) Classification map of Didcot in 2013.

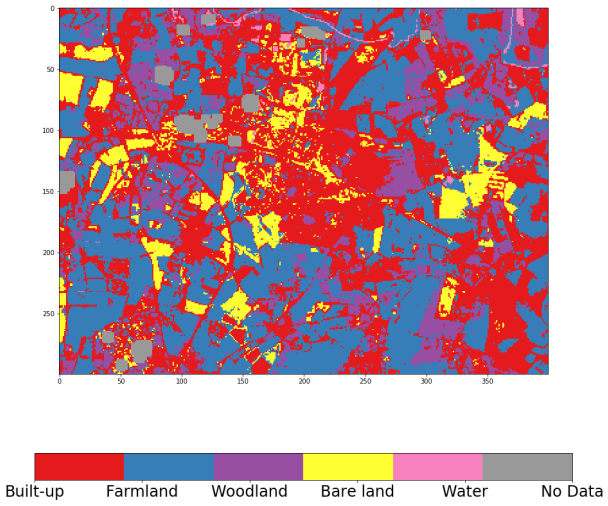

(b) Classification map of Didcot in 2015.

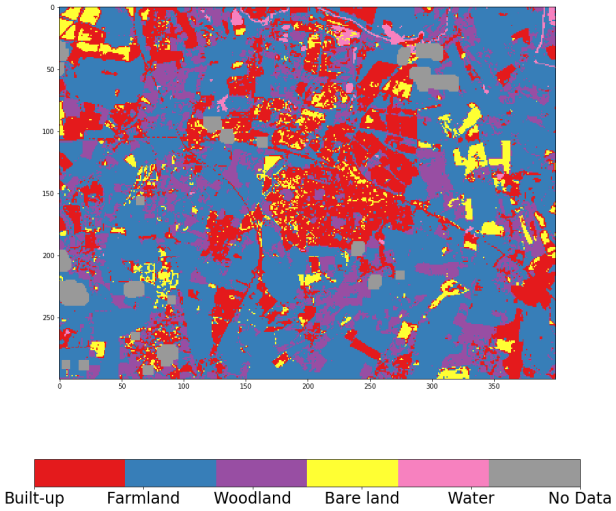

(c) Classification map of Didcot in 2018.

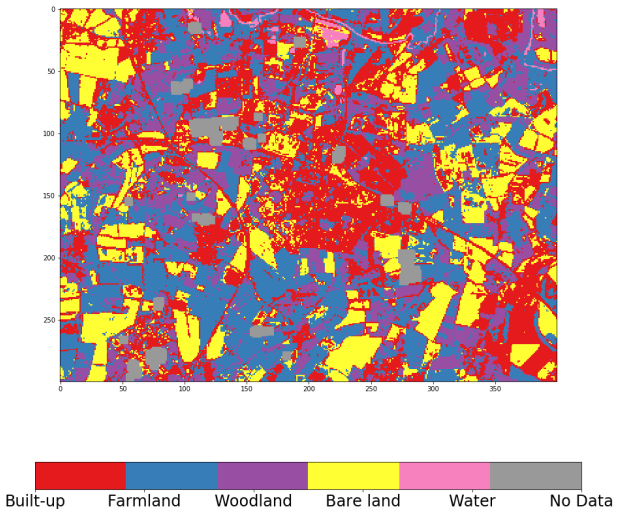

(d) Classification map of Didcot in 2020.

Figure 4.2: Comparison of all four classification maps focused on Didcot.

The values for the physical area for each land cover that is shown in the classification

map are contained within Table 4.1. The percentage of the whole image that is taken up by each land cover is included so that relative changes in the area are in put into perspective. Also a net change of the area over the whole seven year period is included. This is a positive or negative percentage that indicates the how the physical area has increased or decreased. For example the built-up land cover increases from 18.56 km^2 to 33.38 km^2 which is an increase of 80%, and so the net change is +80%.

Class Name	**2013 Area (km^2)**	**%**	**2015 Area km^2**	**%**	**2018 Area (km^2)**	**%**	**2020 Area (km^2)**	**%**	**Net Change of Area (%)**
Built-up	18.56	17.19	43.81	40.56	24.82	22.98	33.38	30.91	+80
Farmland	61.50	56.95	38.66	35.80	54.49	50.46	31.76	29.40	-48
Woodland	21.06	19.50	13.44	12.44	18.82	17.47	18.62	17.24	-12
Bare Land	4.79	4.43	9.30	8.61	5.95	3.51	20.57	19.05	+329
Water	1.32	1.22	2.03	1.88	2.85	2.64	2.71	2.51	+105

Table 4.1: Table showing the calculated area of land cover for each class and each year extrapolated from the classification maps.

The classification map for 2015 claims a large increase in the built-up areas in the image, from 18.56 km^2 to 43.81 km^2. This value then falls to 24.82 km^2 in the next frame. Observing this kind of change in built-up areas cannot be possible within the 2 - 5 year time frame. Therefore this classification can be considered as a failed classification as it has very low accuracy on the focal class (built-up/urban areas). When taking the considerable drop in the farmland area between the same years in question (61.50 km^2 to 38.66 km^2) into account as well, it seems likely that the classifier has mistaken a sizeable proportion of the farmland for built-up areas. Seeing as the images that were used for the 2015 classification came from 9^{th} of April, it is very possible for there to have been hot, dry weather that dried out some of the fields. Comparing the 2015 and 2013 true colour images does show that 2015 seems to be much drier. Although dried out fields should have been classified as bare lands as is noticeable in 2020 which was also taken in April during very dry weather. From inspecting some of the locations of the false classification of the built-up areas, it seems that the colours of the dry fields were more similar to that of some of the built-up areas than the bare lands that I had selected to teach the model. Perhaps including more pixel clusters from less healthy farmland would have improved the accuracy of the 2015 classification. In addition, the data for farmland in 2020 is much lower than 2018 and 2013 but is similar to 2015. This is due to the very dry weather at the time that the image was captured which has caused many of the fields to be classified as bare land. Therefore the data from 2018 should be used when calculating the overall change land use of farmland since 2013, instead of 2020.

Figure 4.3 shows the area of each class changing over time as a percentage of the whole image. The built-up areas can be seen to increase by 80% during the seven year period. The value in 2015 does not fit the trend of gradual increase and can be ignored as the anomalous value is due to poor classification. The farmland trends in a zig-zag fashion which is indicative of the changes in the climate that are present in alternating years. Images from both 2015 and 2020 were taken from mid April when there is usually a period of hot and dry weather. The dry land in 2015 led to a confusion in the classification between farmland and built-up areas. However in 2020, a large amount of farmland had qualified as bare land because it was so dry. This can clearly be seen by the increase in bare land in 2020. Woodland remains relatively constant throughout as it is not affected much by the

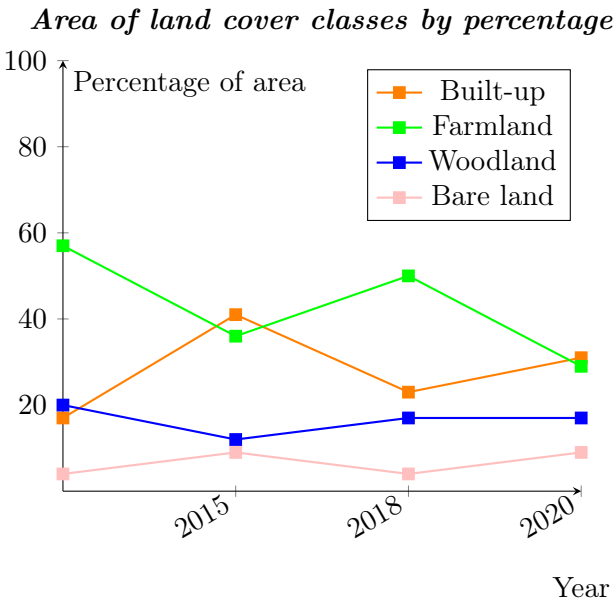

Figure 4.3: A graph showing the relative changes of each class of land cover in percentages of the overall area from 2013 to 2020.

growth of built-up areas.

4.3 Accuracy of Classification

A confusion matrix (see Table 4.2) was computed using the test values and the predicted values created by the model to gain some understanding of the performance of the classification model. The matrix compares the true classes of the pixels against the model's prediction of them. For example, the first cell of the table states that 127 data points were correctly predicted by the model as being a pixel representing a built-up area. Whereas, the value in the fourth row and first column states that 1 data point, that was actually bare land, was predicted to be built-up. A perfectly accurate model would have a confusion matrix where only the diagonal is populated by non-zero values as this would mean all predictions lined up with the actual classes. An accuracy score of 97.6% was calculated for the model used in this project, showing it has effective predicting power. This may change if more training data is supplied to the model.

		Predicted					
		Built-up	**Farmland**	**Woodland**	**Bare land**	**Water**	**No Data**
Actual	Built-up	127	1	0	7	0	0
	Farmland	0	445	0	4	0	0
	Woodland	0	5	11	0	0	0
	Bare land	1	0	0	95	0	0
	Water	0	0	0	0	54	0
	No Data	0	0	0	0	0	9

Table 4.2: Table showing the confusion matrix associated with the training model.

Classification reports compute multiple metrics that describe different ways in which the model has been accurate with it's predictions for each class. It uses true negatives,

false negatives, true positives and false positives as the basis for all computations. True positive is when a case is positive and predicted positive, whereas a false positive is when a case is negative and predicted positive. Precision is a measure of how many predictions were correct which can be looked at by it's ability to not label an instance positive when it is in fact negative. Recall is a measure of how many true positive instance were found out of all positives. So the fewer false negatives (positive instances that have been predicted to be positive) there are, the higher the recall value will be. Finally, the F1 score is a weighted harmonic mean of precision and recall that measures a ratio of how many positive predictions were correct (Krishnan, 2018). All of these metrics are computed and presented in the classification report that can be seen in Table 4.3.

	Precision	Recall	F1 Score
Built-up	0.99	0.94	0.97
Farmland	0.99	0.99	0.99
Woodland	1.00	0.69	0.81
Bare land	0.90	0.99	0.94
Water	1.00	1.00	1.00
No Data	1.00	1.00	1.00

Table 4.3: Classification Report that shows precision, recall and f1 score for each class. Each of these is a metric that comments on the effectiveness of the model.

Looking at the F1 score for all classes (except woodland), the values are in the in 90s meaning that they are nearly 100% correct. Woodland has an F1 score of 0.81, which is little smaller than the others. This is probably due to the very low amount of training data used for that particular class. Only 16 data points were used which is much less than the amounts used for other classes. Woodland is very sparse in the images and so not many samples were taken, however including more should increase this lower performance on the woodland class. Although, this does not affect the classification very significantly since there is not a lot present in the images.

4.4 NDVI Analysis

Visualisation of the NDVI has been effective as can be seen in the Figure 4.4. The healthier crop fields can clearly be seen as they are brightly coloured yellow/green. On the other hand, the darker patches show the unhealthy fields that assist the other images in discerning which years had drier fields. The NDVI in 2015 and 2020 clearly shows more dark patches than 2013 and 2018 which means less healthy crop fields. This supports the likelihood that a large amount of farmland was falsely classified (as built-up areas) in 2015 due to not qualifying for one of the two possible classes: farmland or bare land.

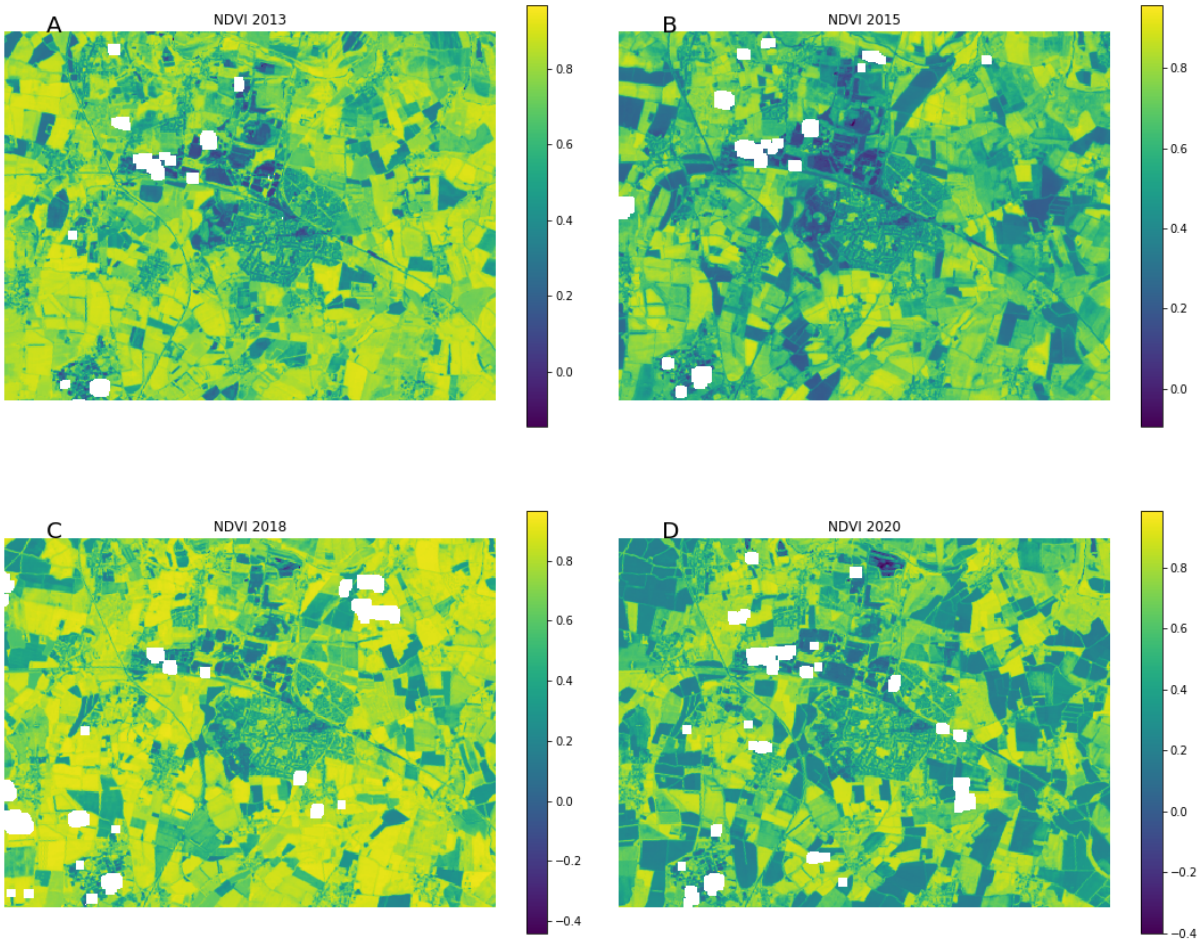

Figure 4.4: Comparison of all four NDVI maps focused on Didcot. A) 2013 B) 2015 C) 2018 D) 2020.

4.5 NDBI Analysis

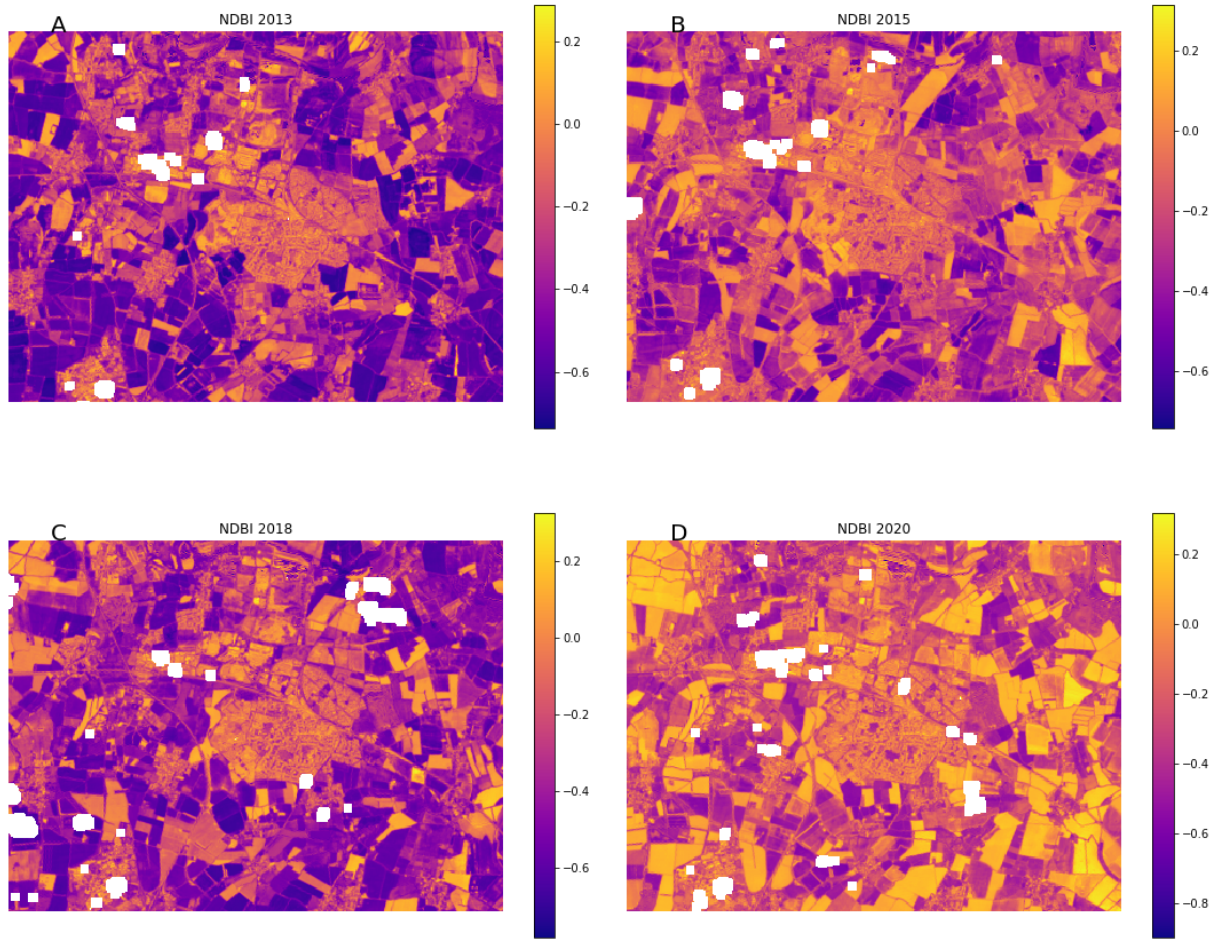

Figure 4.5: Comparison of all four NDBI maps focused on Didcot. A) 2013 B) 2015 C) 2018 D) 2020.

The function of the NDBI is to enhance built-up areas in an image so that they can be seen clearly and so the visualisations should be the opposite of the NDVI. Brighter colours usually represent man-made land covers that constitute built-up areas, whereas darker patches are vegetation and other natural environments. However some dry land covers that are not necessarily man-made can appear as a bright patch on the NDBI. For example, the dry, empty fields west and north-west of the centre in the 2020 frames are bright in the NDBI. Construction of residential areas in the south-western sector of Didcot can be seen developing over the years (see Figure 4.5).

4.6 MNDWI Analysis

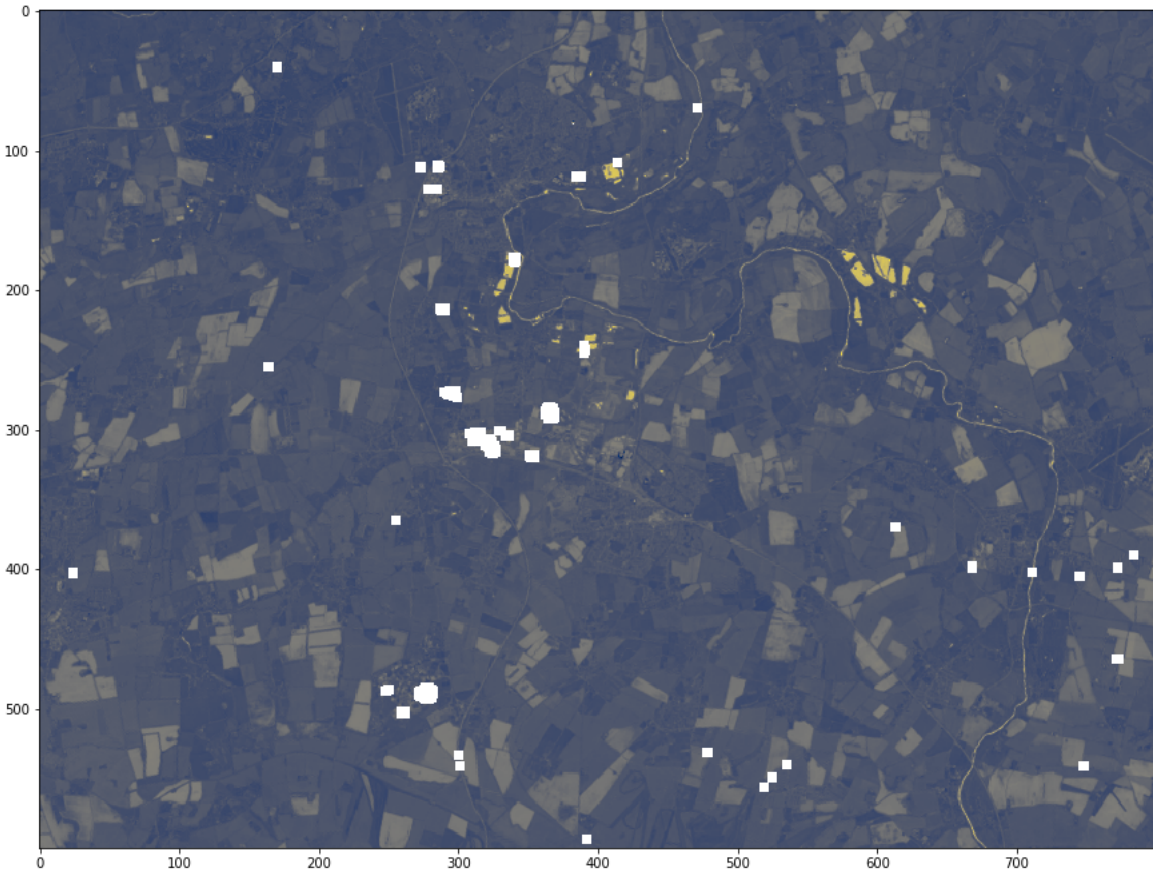

Figure 4.6: The MNDWI visualisation for a larger area around Didcot in 2013.

There is no apparent change in the MNDWI over the whole eight year period. Zooming out of Didcot to a wider view of, the MNDWI can be seen to highlight some bodies of water lining the River Thames that runs through the image, as well as the river itself (see Figure 4.6). These open water bodies are likely to be artificial lakes or reservoirs and were initially being treated as unclear pixels and so were classed as no data. After inspecting the MNDWI, the water bodies were noticed and added to the classification for the water land cover which made them become successfully classed as water. Adding the MNDWI was very helpful for the classification as the water in the image is largely correctly classed.

Chapter 5

Interpretation

5.1 Population and Infrastructure

As urban areas grow, so will the population, leading to a heavier flow of traffic on the roads and a higher demand for public transport. Didcot train station is a key junction into large towns and cities such as, Oxford, Reading and Swindon. So it is likely that in coming years the amount of people using the roads and the public transport will increase quite significantly. Local population of Didcot has increased from 26,920 in 2011 to 30,120 in 2018 and is projected, with a large amount of residential development plans, to reach 62,000 by 2031 (Council, 2020). To support this surge, stronger infrastructure will need to put in place, such as more roads and expansions to public transport.

5.1.1 Harwell Campus

Near the village of Harwell, located approximately 3km from Didcot is where the Harwell Campus is located. This is one of the most important centres for science research and innovation in the United Kingdom. It is home to many major organisations such as Rutherford Appleton Laboratories (RAL) and European Space Agency (ESA). The site has been around since the Second World War and has steadily been growing since. Today it has around 6000 people working within it and so is already a major factor that stimulates a lot of residential growth in the area. Furthermore, the site has a large expansion plan that would expand the area of the site by at least two million square feet. Expansion on existing sectors and creation of new ones, along with a new residential district will without a doubt stimulate a lot of growth in all sectors in the area. The expansion is believed to bring tens of thousands of people into the site (Harwell Campus, 2020). This will cause a substantial increase of urban area land cover in the site and most likely in the surrounding areas as well. A further significant stress on infrastructure will happen as a result of all this development.

5.1.2 Potential Planning Policies

Looking forward to the future, it is reasonable to assume that the footprint of the town of Didcot and the surrounding urban areas will increase quite significantly. Built-up areas have steadily been increasing and will continue to do so as the industries of the area grow. There is plenty of room to grow laterally across the land, as long as destruction of fields does not have any significant knock-on effects. The conversion of fields and farmland into built-up areas will have to be considered intelligently as adverse effects on local agriculture could potentially be an issue for the communities. New developments may consider using more vertical construction to avoid having to build on the fertile land that surrounds the town.

5.2 Better Classification

To make the classification for 2015 more successful, a unique class extraction would have to be made to adjust for the awkward characteristics of the image. This would mean training the model with different data which may not be appropriate for the other images. Future images of Didcot that are similar to the one from 2015 should be considered carefully before being used. Perhaps having a larger pool of training data, specifically a wider range of pixels from the farmland class to account for drier fields that might be mistaken for built-up areas, would benefit the classification for images. Moreover, avoiding images taken from April may be wise as this month often has dry and hot weather that may disrupt the classification.

The pixel-based classification that was used in this project performed to a satisfactory accuracy. Even though the model had an accuracy score of 97.6%, there were many mistakes made in the classification that were noticeable just from inspection. With a higher percentage of accuracy in the classifications, more reliable results and interpretations can be made. If this work was to be furthered, perhaps OBIA could be considered as an alternative to pixel-based. Multiple studies have shown that OBIA retruns a higher level of accuracy in its results because of its more sophisticated machine learning techniques. Zerrouki and Bouchaffra, 2014 found object-based methods to be more accurate in the presence of "a perfect segmentation task prior to object-based classification" and when the number of pixels allowed to define a region was less than eight. A paper published in 2010 carried out a comparative investigation on multi-resolution imagery using pixel-based and object-based methods. Results showed that the object-based approaches were superior in accuracy (82%) and also heavily depended upon the resolution of the images (Weih and Riggan, 2010).

Another factor that could increase accuracy of classification may be the resolution of the fundamental images that are used. Band 8 of landsat 8 data is the panchromatic band. This produces a black and white image with a resolution of 15m, magnifying the resolution of other bands by a factor of four. This data can be combined with other bands to achieve higher resolution images that can be used in classification. Band 8 was not available using the earthexplorer.usgs.gov and so was not included in the files downloaded for this project. Obtaining higher accuracy with classifications would make this type of data more reliable for its many applications within the scope of monitoring urban development. Therefore using images of higher resolution alongside more intelligent machine learning techniques be a definite improvement for future works.

Chapter 6

Conclusion

The classification maps for 2013, 2018 and 2020 were successful because they managed to classify land cover accurately and produced useful information. Classification for 2015 was regarded as a failure due to the significant overestimate of the built-up land cover. Ultimately this was caused by characteristics of the image that were dependent on the conditions of the land. Apart from that, analysis of the data fit expectations as urban areas were seen to grow 80%. The methods used could be repeated for future years as growth is predicted to accelerate which may mean that more monitoring is needed. Although higher resolution images and more sophisticated machine learning techniques could be employed for more accurate and reliable results.

With more time I would have liked to explore more advanced machine learning techniques such as OBIA and seen how much more superior they were at classifying my selected area. Also I would have perhaps tried to used these techniques on larger urban areas such as cities in developing countries. Developing countries are usually warmer which would benefit the selection of images from Landsat since the cloudy climate of the UK limited the range of images that were available. In addition, urban areas in developing countries have more need for this sort of technology to be used for them as planning is key as they experience rapid growth.

Acknowledgements

Thank you to PhD student Edward Salakpi for helping so much with this project and Prof Seb Oliver for supervising me.

Bibliography

ArcGIS (2020). *Sentinel-2 Imagery: Normalized Difference Built-Up Index (NDBI)*. URL: https://www.arcgis.com/home/item.html?id=3cf4e98f035e47279091dc74d43392a5.

Al-Bilbisi, Hussam (2019). "Spatial Monitoring of Urban Expansion Using Satellite Remote Sensing Images: A Case Study of Amman City, Jordan". In: *Sustainability* 11. URL: https://www.researchgate.net/publication/332435773%7B%5C_%7DSpatial%7B%5C_%7DMonitoring%7B%5C_%7Dof%7B%5C_%7DUrban%7B%5C_%7DExpansion%7B%5C_%7DUsing%7B%5C_%7DSatellite%7B%5C_%7DRemote%7B%5C_%7DSensing%7B%5C_%7DImages%7B%5C_%7DA%7B%5C_%7DCase%7B%5C_%7DStudy%7B%5C_%7Dof%7B%5C_%7DAmman%7B%5C_%7DCity%7B%5C_%7DJordan.

Council, South Oxford District (2020). *About Didcot*. URL: http://www.southoxon.gov.uk/services-and-advice/business/support-businesses/already-doing-business-area/town-centre-vitality/d-2.

Geography, GIS (2020). *Supervised and Unsupervised Classification in Remote Sensing*. URL: https://gisgeography.com/supervised-unsupervised-classification-arcgis/.

Harwell Campus (2020). *Our Vision*. URL: https://www.harwellcampus.com/vision/.

Krishnan, Muthu (2018). *Understanding the Classification report through sklearn*. URL: https://muthu.co/understanding-the-classification-report-in-sklearn/.

Kshetri, Tek (2018). *NDVI, NDBI & NDWI Calculation Using Landsat 7, 8*. URL: https://www.linkedin.com/pulse/ndvi-ndbi-ndwi-calculation-using-landsat-7-8-tek-bahadur-kshetri.

McFEETERS, S K (1996). "The use of the Normalized Difference Water Index (NDWI) in the delineation of open water features". In: *International Journal of Remote Sensing* 17.7, pp. 1425–1432. DOI: 10.1080/01431169608948714. URL: https://doi.org/10.1080/01431169608948714.

Ming, Dongping et al. (2016). "Land cover classification using random forest with genetic algorithm-based parameter optimization". In: *Journal of Applied Remote Sensing* 10, p. 35021. DOI: 10.1117/1.JRS.10.035021.

NASA (2000). *Measuring Vegetation (NDVI & EVI)*. URL: https://earthobservatory.nasa.gov/features/MeasuringVegetation/measuring%7B%5C_%7Dvegetation%7B%5C_%7D2.php.

— (2020). *Landsat 8*. URL: https://landsat.gsfc.nasa.gov/landsat-data-continuity-mission/.

Patel, S (2017). *Chapter 5: Random Forest Classifier*. URL: https://medium.com/machine-learning-101/chapter-5-random-forest-classifier-56dc7425c3e1.

Phiri, Darius and Justin Morgenroth (2017). "Developments in Landsat Land Cover Classification Methods: A Review". In: *Remote Sensing* 9.9. URL: https://www.mdpi.com/2072-4292/9/9/967.

United Nations (2019a). *Special edition: progress towards the Sustainable Development Goals*. Tech. rep. URL: https://undocs.org/E/2019/68.

— (2019b). *World Population Prospects 2019*. Tech. rep., p. 5. URL: https://population.un.org/wpp/Publications/Files/WPP2019%7B%5C_%7DHighlights.pdf.

United Nations (2020). *Sustainability*. URL: https://academicimpact.un.org/content/sustainability (visited on 05/15/2020).

Weih, Robert C and Norman D Riggan (2010). "Object-based classification vs. Pixel-based classification: Comparitive importance of multi-resolution imagery". In: *International Archives of the Photogrammetry, Remote Sensing and Spatial Information Sciences - ISPRS Archives* 38.

Xie, Z. et al. (2019). "Classification of Land Cover, Forest, and Tree Species Classes with ZiYuan-3 Multispectral and Stereo Data". In: *Remote Sensing* 11. URL: https://doi.org/10.3390/rs11020164.

Xu, Hanqiu (2006). "Modification of Normalized Difference Water Index (NDWI) to Enhance Open Water Features in Remotely Sensed Imagery". In: *International Journal of Remote Sensing* 27, pp. 3025–3033. DOI: 10.1080/01431160600589179.

Zerrouki, N. and D. Bouchaffra (2014). "Pixel-based or Object-based: Which approach is more appropriate for remote sensing image classification?" In: *2014 IEEE International Conference on Systems, Man, and Cybernetics (SMC)*, pp. 864–869. DOI: 10.1109/SMC.2014.6974020.